

**ANNALS OF THE UNIVERSITY OF CRAIOVA  
ANNALES DE L'UNIVERSITÉ DE CRAIOVA**

---

---

**ANALELE  
UNIVERSITĂȚII  
DIN CRAIOVA**

**SERIA: INGINERIE ELECTRICĂ  
SERIE: ELECTRICAL ENGINEERING  
SÉRIE: INGÉNIERIE ÉLECTRIQUE**

**Anul/Year/Année 44  
No. 44, Vol. 44, Issue 1, 2020**

**December 2020**

---

---

**ISSN 1842 - 4805**

**EDITURA UNIVERSITARIA**

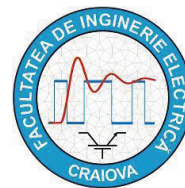
---

---

# ANNALS OF THE UNIVERSITY OF CRAIOVA



13, A.I. Cuza Str., CRAIOVA 200585  
ROMANIA



---

**We exchange publications  
with similar institutions of country and from abroad**

## ANNALES DE L'UNIVERSITÉ DE CRAIOVA

Rue A.I. Cuza, No. 13, CRAIOVA 200585  
ROUMANIE

---

**On fait des échanges des publications  
avec les institutions similaires du pays et de l'étranger**

---

---

**This journal is published by the Faculty of Electrical Engineering from the University of Craiova.  
The authors are fully responsible for the originality of their papers and for accuracy of their notes.**

### Editorial board

Prof.dr.ing. Ioan POPA editor in chief, University of Craiova, Romania  
Conf.dr.ing. Mircea DRIGHICIU - editor in chief, University of Craiova, Romania  
Prof.dr.ing. Dan MIHAI, University of Craiova, Romania  
Prof.dr.ing. Marian CIONTU, University of Craiova, Romania  
Prof.dr.ing. Sergiu IVANOV, University of Craiova, Romania  
Prof.dr.ing. Lucian MANDACHE, University of Craiova, Romania  
Prof.dr.sc. Ivan YATCHEV, Technical University of Sofia, Bulgaria  
Prof.dr.ing. Leszek CZARNECKI, Life Fellow IEEE, Louisiana State University, USA  
Prof.dr.ing. Slavoljub ALEKSIC, University of Nic, Serbia  
Prof.dr.ing. Sergey RYVKIN, Control Sciences Institute "V.I.Trapeznikov", Russia  
Prof.dr.ing. Mihai IORDACHE, University "Politehnica" of Bucharest, Romania  
Prof.dr.ing. Victor ŞONTEA, Technical University of Moldova, Moldova  
Prof.dr.ing. Iuliu DELEŞEGA, University "Politehnica" of Timișoara, Romania  
Prof.dr.ing. Dumitru-Marcel ISTRATE, "Gh. Asachi" Technical University of Iași, Romania  
Prof.dr.ing. Miroslav PRSA, University of Novisad, Serbia  
Prof.dr.ing. Maria BROJBOIU, University of Craiova, Romania  
Prof.dr.ing. Mihai GAVRILAŞ, "Gh. Asachi" Technical University of Iași, Romania  
Prof.dr.ing. Daniela DANCIU, University of Craiova, Romania  
Prof.dr.ing. Nicolae MUNTEAN, University "Politehnica" of Timișoara, Romania  
Prof.dr.ing. Călin MUNTEANU, Technical University of Cluj-Napoca, Romania  
Prof.dr.ing. Leonardo-Geo MĂNESCU, University of Craiova, Romania  
Prof.dr.ing. Camelia PETRESCU, "Gh. Asachi" Technical University of Iași, Romania  
S.I.dr.ing. Ioana Gabriela SÎRBU, University of Craiova, Romania

## REVIEWERS COMMITTEE

Lia-Elena ACIU - *Transilvania University of Braşov, Romania*  
Maricel ADAM – *"Gh. Asachi" Technical University of Iaşi, Romania*  
Mihaela ALBU – *University "Politehnica" of Bucharest, Romania*  
Slavoljub ALEKSIC – *University of Nis, Serbia*  
Horia BĂLAN – *Technical University of Cluj-Napoca, Romania*  
Gheorghe BĂLUȚĂ – *"Gh. Asachi" Technical University of Iaşi, Romania*  
Alexandru BITOLEANU – *University of Craiova, Romania*  
Maria BROJBOIU – *University of Craiova, Romania*  
Emil CAZACU – *University "Politehnica" of Bucharest, Romania*  
Aurel CĂMPEANU – *University of Craiova, Romania*  
Mihai CERNAT – *Transilvania University of Braşov, Romania*  
Marian CIONTU – *University of Craiova, Romania*  
Daniel Cristian CISMARU – *University of Craiova, Romania*  
Grigore CIVIDJIAN – *University of Craiova, Romania*  
Zlata CVETCOVIC – *University of Nis, Serbia*  
Leszek CZARNECKI - *Louisiana State University, USA*  
Daniela DANCIU – *University of Craiova, Romania*  
Sonia DEGERATU – *University of Craiova, Romania*  
Iuliu DELEŞEGA – *University "Politehnica" of Timişoara, Romania*  
Silvia-Maria DIGĂ – *University of Craiova, Romania*  
Peter DINEFF – *Technical University of Sofia, Bulgaria*  
Radu DOBRESCU – *University "Politehnica" of Bucharest, Romania*  
Mircea-Adrian DRIGHICIU – *University of Craiova, Romania*  
Laurentiu Marius DUMITRAN – *University "Politehnica" of Bucharest, Romania*  
Sorin ENACHE – *University of Craiova, Romania*  
Virgiliu FIRETEANU – *University "Politehnica" of Bucharest, Romania*  
Dan FLORICĂU – *University "Politehnica" of Bucharest, Romania*  
Cristian FOŞALĂU – *"Gh. Asachi" Technical University of Iaşi, Romania*  
Teodor Lucian GRIGORIE – *Military Technical Academy "Ferdinand I", Romania*  
Micea-Dan GUSA – *"Gh. Asachi" Technical University of Iaşi, Romania*  
Stefan HĂRĂGUŞ – *University "Politehnica" of Timişoara, Romania*  
Elena HELEREA – *Transilvania University of Braşov, Romania*  
Eugen HNATIUC – *"Gh. Asachi" Technical University of Iaşi, Romania*  
Kemal HOT – *Polytechnic of Zagreb, Croatia*  
Eugen IANCU – *University of Craiova, Romania*  
Nathan IDA – *University of Akron, USA*  
Maria IOANNIDES – *National Technical University of Athens, Greece*  
Valentin IONIȚĂ – *University "Politehnica" of Bucharest, Romania*  
Mihai IORDACHE – *University "Politehnica" of Bucharest, Romania*  
Marcel ISTRATE – *"Gh. Asachi" Technical University of Iaşi, Romania*  
Sergiu IVANOV – *University of Craiova, Romania*  
Virginia IVANOV – *University of Craiova, Romania*  
Wilhelm KAPPEL – *National Research and Development Institute for Electrical Engineering (ICPE – CA) Bucharest, Romania*  
Liviu KREINDLER – *University "Politehnica" of Bucharest, Romania*  
Gheorghe LIVINȚ – *"Gh. Asachi" Technical University of Iaşi, Romania*  
Dumitru Dorin LUCHACHE – *"Gh. Asachi" Technical University of Iaşi, Romania*  
Lucian MANDACHE – *University of Craiova, Romania*  
Gheorghe MANOLEA – *University of Craiova, Romania*

Andrei MARINESCU – *Romanian Academy of Technical Science, Craiova Branch, Romania*  
Iliana MARINOVA – *Technical University of Sofia, Bulgaria*  
Claudia MARTIȘ – *Technical University of Cluj-Napoca, Romania*  
Ernest MATAGNE – *Université Catholique de Louvain, Belgium*  
Leonardo-Geo MĂNESCU – *University of Craiova, Romania*  
Dan MIHAI – *University of Craiova, Romania*  
Alexandru MOREGA – *University “Politehnica” of Bucharest, Romania*  
Mihaela MOREGA – *University “Politehnica” of Bucharest, Romania*  
Nazih MOUBAYED – *Lebanese University, Lebanon*  
Călin MUNTEANU – *Technical University of Cluj-Napoca, Romania*  
Florin MUNTEANU – *"Gh. Asachi" Technical University of Iași, Romania*  
Valentin NĂVRĂPESCU – *University “Politehnica” of Bucharest, Romania*  
Mitică Iustinian NEACĂ – *University of Craiova, Romania*  
Ciprian NEMEȘ – *"Gh. Asachi" Technical University of Iași, Romania*  
Petre-Marian NICOLAE – *University of Craiova, Romania*  
Dragoș NICULAE - *University “Politehnica” of Bucharest, Romania*  
Petru NOTINGHER – *University “Politehnica” of Bucharest, Romania*  
Teodor PANĂ – *Technical University of Cluj-Napoca, Romania*  
Camelia PETRESCU – *"Gh. Asachi" Technical University of Iași, Romania*  
Ioan POPA – *University of Craiova, Romania*  
Dan POPESCU – *University of Craiova, Romania*  
Daniela POPESCU – *University of Craiova, Romania*  
Mihaela POPESCU – *University of Craiova, Romania*  
Miroslav PRSA – *University of Novi-Sad, Serbia*  
Mircea M. RĂDULESCU – *Technical University of Cluj Napoca, Romania*  
Victorița RĂDULESCU - *University “Politehnica” of Bucharest, Romania*  
Benoit ROBYNS – *Ecole des Hautes Etude d'Ingénieur de Lille, France*  
Constantin ROTARU – *Military Technical Academy "Ferdinand I", Romania*  
Alex RUDERMAN – *Elmo Motion Control Ltd, USA*  
Sergey RYVKIN – *Trapeznikov Institute of Control Sciences, Russia*  
Alexandru SĂLCEANU – *"Gh. Asachi" Technical University of Iași, Romania*  
Cristina Gabriela SĂRĂCIN – *University “Politehnica” of Bucharest, Romania*  
Constantin SĂRMAȘANU – *"Gh. Asachi" Technical University of Iași, Romania*  
Dan SELIȘTEANU – *University of Craiova, Romania*  
Victor ȘONTEA – *Technical University of Moldova, Moldova*  
Alexandru STANCU – *"A.I. Cuza" University of Iași, Romania*  
Viorel STOIAN – *University of Craiova, Romania*  
Ryszard STRZELECKI – *University of Technology Gdansk, Poland*  
Flavius-Dan ȘURIANU – *University “Politehnica” of Timișoara, Romania*  
Lorand SZABO – *Technical University of Cluj-Napoca, Romania*  
Radu-Adrian TÎRNOVAN – *Technical University of Cluj-Napoca, Romania*  
Raina TZENEVA – *Technical University of Sofia, Bulgaria*  
Ioan VADAN – *Technical University of Cluj-Napoca, Romania*  
Viorel VARVARA – *"Gh. Asachi" Technical University of Iași, Romania*  
Ion VLAD – *University of Craiova, Romania*  
Ivan YATCHEV – *Technical University of Sofia, Bulgaria*

# The Use of Helmholtz Coils Designed for 50 Hz at Higher Frequencies

Georgiana Roşu<sup>\*</sup>, Ionel Dumbravă<sup>†</sup>, Ion Pătru<sup>†</sup>, Aurelia Scornea<sup>†</sup>, Octavian Baltag<sup>§</sup>, Andrei Marinescu<sup>#</sup>

<sup>\*</sup> Military Technical Academy, George Cosbuc Blv. 39-49, Bucharest 050141, Romania, [georgianamarin01@gmail.com](mailto:georgianamarin01@gmail.com)

<sup>†</sup> R&D National Institute ICMET Craiova, Decebal Blv. 118A, Craiova 200746, Romania, [icmet@icmet.ro](mailto:icmet@icmet.ro)

<sup>§</sup> Faculty of Medical Bioengineering – UMF, Iasi, Romania, [octavian.baltag@bioinginerie.ro](mailto:octavian.baltag@bioinginerie.ro)

<sup>#</sup> ASTR, Craiova Branch, 107 Decebal Av., Craiova 200440, Romania, [ancor2005@gmail.com](mailto:ancor2005@gmail.com)

**Abstract** - Helmholtz coils (HC) are used in order to generate and control uniform magnetic fields for a variety of research applications. They can be easily constructed and their fields can be easily calculated. This makes them especially useful in calibrating magnetic field sensors. Such a calibration system with large Helmholtz coils (1x1m) can be found in ICMET Institute, designed to operate only at a frequency of 50 Hz. There has recently been a request for the calibration of several measuring sensors operating at frequencies up to 10 kHz used in industrial applications such as induction hardening of metal parts. The paper aims to determine the conditions under which this low frequency HC system can be used at frequencies at least 100 times higher. The first part of the paper describes a theoretical analysis on the volume confining the space where the magnetic field components have a predetermined deviation (a 2% threshold) from the center of the HC system followed by a comparison with a 3D FEM simulation and measurement of HC field. The second part describes the identification of the HC parameters at higher frequencies and the resonant methods used to achieve the excitation power required at these frequencies.

**Cuvinte cheie:** bobine Helmholtz, parametri, sursă rezonantă, model FEM, volum de câmp uniform.

**Keywords:** Helmholtz coils, parameters, resonant supply, FEM model, uniform field volume.

## I. INTRODUCTION

The precise measurement of the magnetic fields generated by electrical and electronic equipment is a requirement imposed by international standards. In some cases, it includes functional measurements; in other cases, there are safety measures imposed for the general public or operators. Periodic calibration of the equipment and sensors for the magnetic field measurement is imposed by the laboratory quality assurance system. However, the cost of such calibration is substantial due to the small number of laboratories accredited for this type of measurements.

Such a calibration system with Helmholtz coils can be found in ICMET Institute, operating at a frequency of 50 Hz and the respective measurement was accredited in 2007 by DKD (Deutscher Kalibrierdienst) [1].

ICMET Institute has recently received several requests for the calibration of certain sensors operating at frequencies up to 10 kHz, needed for example, for magnetic measurements in industrial applications such as induction hardening of metal parts.

The paper aims to answer the question of whether the existing HC system can operate at frequencies at least 100 times higher than 50 Hz and under what conditions.

First the paper presents a theoretical analysis of the HC system which determines the region confined by a predetermined deviation of the magnetic field components related to the magnetic field value in the centre of the Helmholtz system. Also related to the theoretical elements, the paper determines the dependence of the “field uniformity volume” (with predetermined deviation of field values) to the distance between the two coils of the Helmholtz system.

The Helmholtz system analysis [2 - 4] is extended to the use of simulation software based on the finite element method. By implementing the three-dimensional geometric model of the Helmholtz system in the Ansys Maxwell virtual environment, there are obtained the magnetic field values, computed in the space area confined by the rectangular HC system. The dimensions of the field uniformity volume characterising the Helmholtz coils system located at ICMET [5] are determined based on the results of the numerical simulation.

Then the paper describes the HC parameters identification at higher frequencies (self resonance, AC resistance, parasitic capacitance of the coils etc), necessary to obtain an equivalent diagram of HC system. The circuit simulation with LT Spice software confirms the possibility of using the existing HC system at high frequencies below the resonant frequency of the system. The power supply of the system is presented in a series resonance circuit and the simulation of this circuit is compared with the experimental results.

## II. THEORETICAL ASPECTS OF HELMHOLTZ SYSTEMS

In order to determine the magnetic field generated by the Helmholtz system, the contributions of the eight current segments constituting the sides of the two coils composing the HC model were considered. The well-known conditions for gradient annulment in the system’s geometric centre were imposed, to achieve the uniformity condition. The following parameters were taken into account: the coils sides are considered segments of length  $a$ , carrying an electric current of intensity  $I$ , and the coils located at distance  $d/2$ . Thus, the following relationship is obtained for determining the magnetic field induction generated by one coil [6 - 8]:

$$B(z) = \frac{2\mu_0 I a^2}{\pi} \left( \frac{1}{\sqrt{a^2 + (z-d/2)^2} \sqrt{2a^2 + (z-d/2)^2}} + \frac{1}{\sqrt{a^2 + (z+d/2)^2} \sqrt{2a^2 + (z+d/2)^2}} \right) \quad (1)$$

For the considered Helmholtz system, the length of the coil side is  $a = 1$  m. In order to calculate the deviation of the magnetic flux density from the geometric centre on the  $-z \dots 0 \dots +z$  axis of the coordinate system, an electric current  $I = 1$  A was considered and the magnetic induction results in a dependence on just two parameters  $z$  and  $d$ :

$$B(z, d) = \frac{2\mu_0}{\pi} F(z, d) \quad (2)$$

Fig. 1 shows the plotting the above mentioned function, which determines the relative deviation of the magnetic flux density values  $B(z, d)$ , considering as standard value the magnetic induction  $B_H$  in the geometric centre of a system fulfilling the Helmholtz condition for square coils:

$$\frac{d}{2} = 0.5445a \quad (3)$$

$$\Delta B = \frac{B_H - B(z, d)}{B_H} = \frac{F_H - F(z, d)}{F_H} = 1 - \frac{F(z, d)}{F_H} \quad (4)$$

Fig. 2 illustrates the deviation of the  $F(z, d)$  function compared to its value in the geometric centre  $z = 0$ , considering the distance  $d/2$  as function parameter:

$$F(z, d) - F(z = 0, d) \quad (5)$$

These representations are useful when a particular workspace is concerned, considering a pre-set deviation value in the magnetic field relative to its central value.

Fig. 3 illustrates a detailed view of the previous representation. It is obvious that for smaller distances between the two HC, the magnetic field representation displays a bulge, whereas for larger distances between coils – there are two bulges, indicating larger field gradients. Also, it is noted that the highest precision is achieved while fulfilling the Helmholtz condition – the distance between coils being 0.5445 times the coil side 1 m which corresponds to the HC system analyzed in the paper.

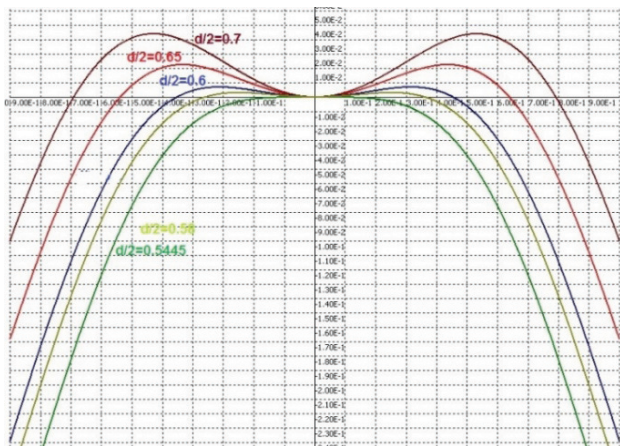


Fig. 1. The magnetic field deviation relative to its value in the geometric center for the Helmholtz coils system.

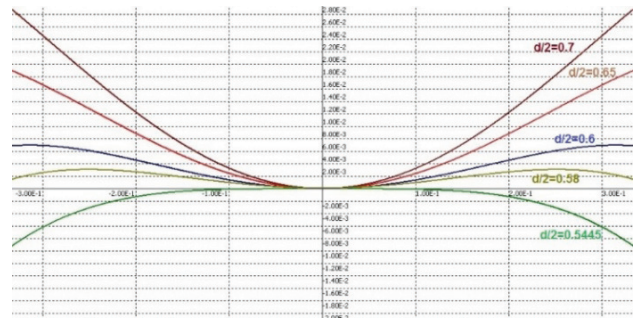


Fig. 2. Deviation of the  $F(z, d)$  function relative to its value in the geometric center.

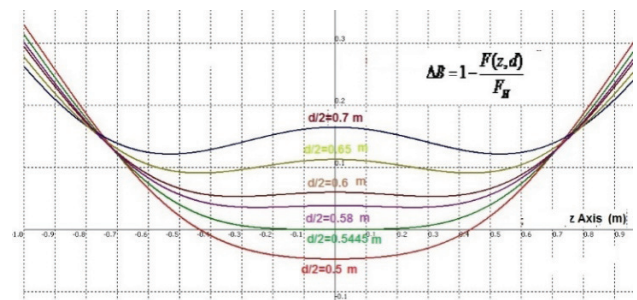


Fig. 3. Detailed view of the deviation of the  $F(z, d)$  function relative to its value in the geometric center.

Therefore, as illustrated in the detailed view in Fig. 3, the longitudinal distance for which the field uniformity is achieved is approximately 200 mm, for the Helmholtz condition.

### III. NUMERICAL SIMULATION RESULTS

The Helmholtz system analysis is extended to the use of simulation software based on the finite element method [9 - 12]. The geometric model of the HC system was implemented in the virtual environment, each coil being comprised of a single turn. The system geometry is illustrated in Fig. 4 where the coil side is  $a = 1$  m, and the distance between coils is 0.5445 m. The coils are marked in purple, and the current excitation – entering and exiting the coils, is marked with red arrows.

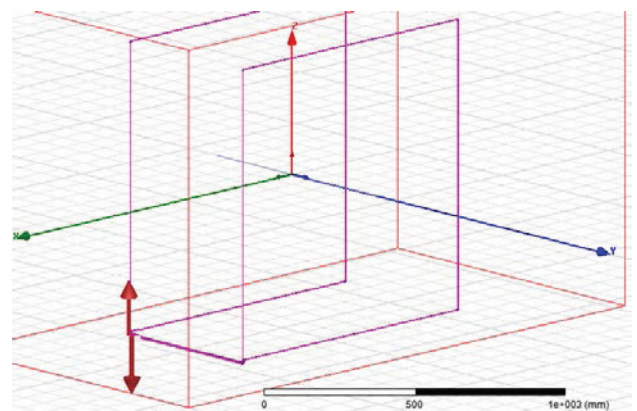


Fig. 4. Geometry of the Helmholtz rectangular coil system.

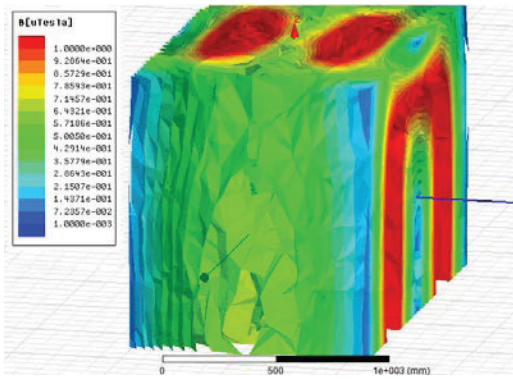


Fig. 5. The magnetic induction generated by the Helmholtz system in the analyzed region.

In order to minimize the impact on the field uniformity of the wire connecting the two rectangular coils, two parallel wires are drawn – one wire connecting the coils and the other returning wire, at a distance of 5 mm.

This small distance between the wires causes a variation between the tangential components of the magnetic field generated by the electric current passing through the wires in opposite directions, which further determines a lower vertical dimension of the volume of the field uniformity [13].

The analysed region is delimited by a rectangular box surrounding the coils. Fig. 5 shows the magnetic field generated by the pair of rectangular coils in Helmholtz configuration carrying an electric current  $I = 1$  A. The electric current excitation is applied at the edges of the coil pair, located on the left side of the system, as detailed in Fig. 4.

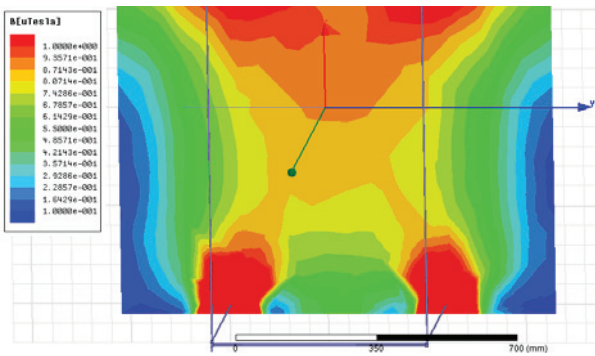


Fig. 6. The longitudinal plane section of the HC field domain.

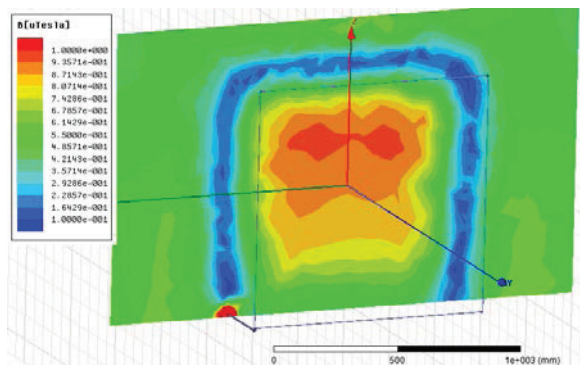


Fig. 7. The transversal plane section of the HC field domain.

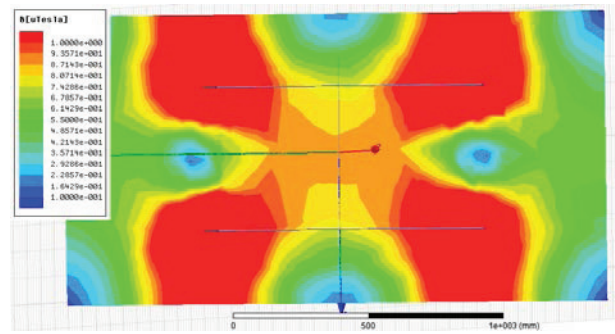


Fig. 8. The horizontal plane section of the HC field domain.

In order to obtain a better view of the magnetic field distribution in the analysed region, and to determine the uniformity region, Figs. 6 - 8, show sections of the region in the longitudinal plane (on the axis of the coils), the transversal plane and the horizontal plane, respectively.

Since the area of interest is located on the axis of the coils – passing through the center of the two coils, the magnetic induction is computed on the above mentioned axis. Fig. 9 illustrates such a representation. Thus, a zone of field uniformity around 200 mm is achieved on the longitudinal axis, corresponding to the theoretical calculations.

By extending the view and achieving better accuracy in expressing the field uniformity, the region of interest is the one determined by the uniform magnetic field relative to the field value in the geometric centre of the HC system.

The normalized difference of the magnetic induction values relative to the standard value of the magnetic induction in the geometric centre is computed, in order to determine the respective region [14, 15].

The deviation of the magnetic field relative to the value in the centre of the HC system (also considered as the centre of the coordinate system) is determined based on the magnetic field values obtained in Figs. 6 - 8. The magnetic field in the centre of the HC system is  $B_0 = 0.888 \mu\text{T}$ .

The relative deviation is computed with relationship:

$$B_{rel}(x, y, z) = \frac{|B(x, y, z) - B_0(0,0,0)|}{B_0(0,0,0)} * 100 [\%] \quad (6)$$

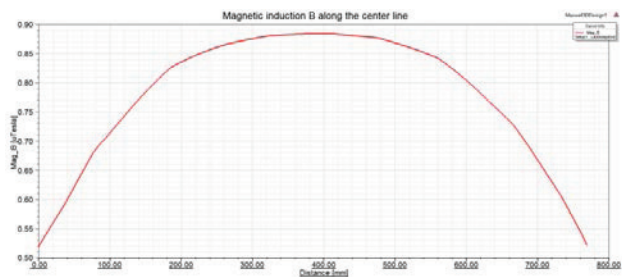


Fig. 9. The magnetic induction computed along the centerline of the Helmholtz system.

The purpose is to determine the region where the magnetic field deviation relative to the centre value is less than 2%. In order to obtain a better view of the field distribution in the analysed region, and to determine the uniform field region, Figs. 10 - 12 show sections of the region in

the longitudinal plane (on the coil pair axis), in the transversal plane and in the horizontal plane, respectively.

Therefore, the illustrations describe the space defined by field uniformity – a deviation less than 2 % relative to the centre field value. As noticed in Fig. 10, on the longitudinal axis (OY), field uniformity is obtained on a distance of 180 mm, slightly shorter than the distance of uniformity of 200 mm obtained based on the analytical calculations and illustrated in Fig. 3.

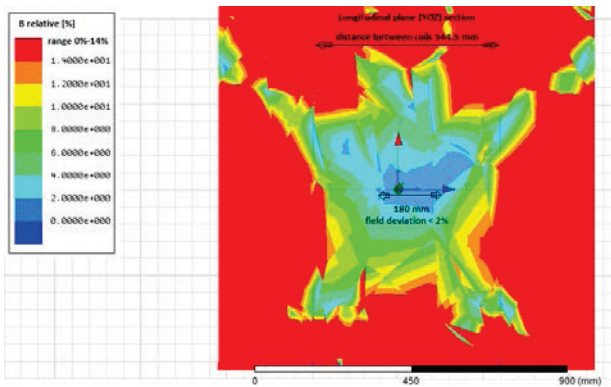


Fig. 10. Field uniformity in the longitudinal plane HC section.

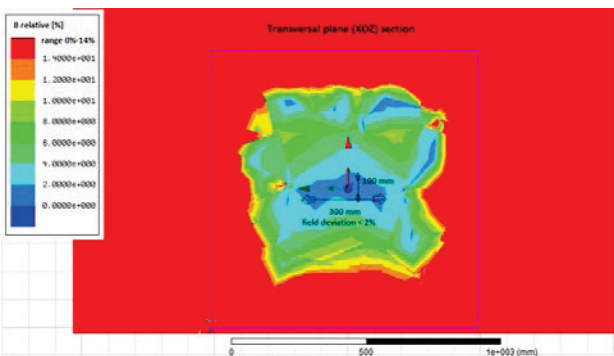


Fig. 11. Field uniformity in the transversal plane HC section.

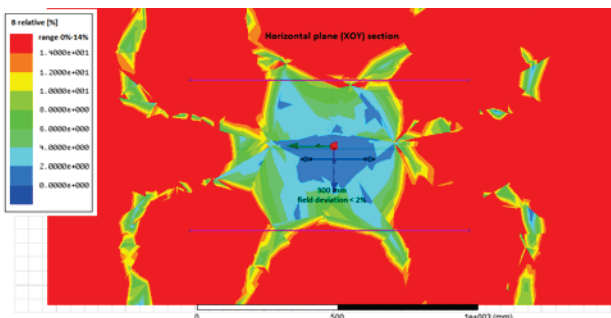


Fig. 12. Field uniformity in the horizontal plane HC section.

TABLE I.  
FIELD UNIFORMITY VOLUMES

Field deviation percentage	Uniform field volume dimensions OX, OY, OZ
1 %	260 mm x 150 mm x 80 mm
2 %	<b>300 mm x 180 mm x 100 mm</b>
5 %	600 mm x 340 mm x 280 mm

Table 1 comprises the dimensions of the uniform field volume for several threshold levels for field deviation to the centre: 1 %, 2 %, and 5 %, respectively.

It is worth mentioning that the simulation model comprised of 1 turn per each coil of the HC system has an inductance of 7.9941  $\mu\text{H}$ , as computed by the Maxwell software.

#### IV. ANALYSIS OF HC SYSTEM

The construction and installation of the HC system with rectangular geometry (Fig. 13), designed initially for the calibration of industrial magnetic probes at frequencies of only 50 Hz, was very convenient. A rectangular HC system generates a volume of nearly uniform magnetic field greater than a circular HC of comparable dimensions [2]. The performance is maintained up to a certain frequency limit. The frequency limitation is a function of the coil's parameters (wire size and type-solid or litz wire-, number of turns and layers), type of connection (series or parallel) of the two coils and finally the supply configuration (balanced or unbalanced with respect to ground).

A Vector Network Analyzer (VNA) device was used for the identification of all circuit parameters (Fig. 14) by impedance and frequency characteristics measurements [16]. The parasitic capacitance  $C_p$  is determined from the first resonance frequency of the coils system. Table 2 contains  $L$ ,  $C_p$ ,  $f_r$  values, and Table 3 contains the AC resistance of the coils for different frequencies. The significant increase of AC resistance is the result of skin and proximity effects in the original solid wire multilayer coils.

The frequency characteristic of the HC is illustrated in Fig. 15. The resonant frequency is  $f_r = 15.6$  kHz, which shows that the maximum working frequency of the HC calibration system must be less than the 10 kHz until the system remains inductive.

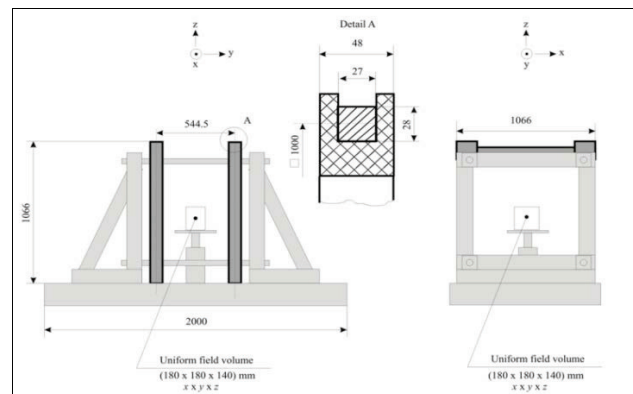


Fig. 13. Design of the Helmholtz coil system.

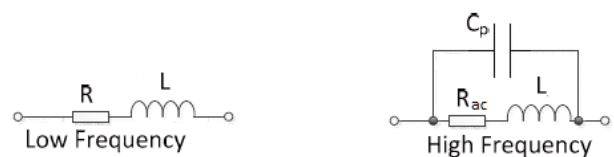


Fig. 14. HC equivalent circuit.

TABLE II.  
MEASURED PARAMETERS OF THE HC SYSTEM.

Parameter	Value
$f_r$	15.6 kHz
$L$	2 x 77 mH/coil
$C_p$	0.675

TABLE III.  
AC RESISTANCE AND QUALITY FACTOR  
DEPENDING ON THE FREQUENCY.

Frequency (Hz)	Rac ( $\Omega$ )	Q
50.44	4.15	5.85
502.95	4.85	50.01
994.13	7.37	65.15
5014	55	44.08

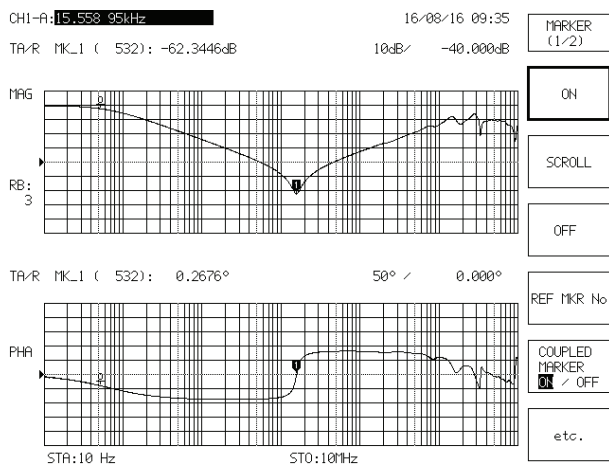


Fig. 15. Frequency characteristic of HC system.

In order to compare the FEM data with the experimental data, it is necessary to perform a review of the HC model in Maxwell software. As specified above, the total inductance of the HC system determined by Maxwell software is 7.9941  $\mu$ H; dividing it by 2, we get the inductance per turn of approximately 4  $\mu$ H. The total number of turns of the actual HC system is 276, meaning there are approximately 138 turns per each coil. By multiplying the inductance of one coil in the Maxwell model by squared number of turns ( $N = 138$ ), we get a total inductance per coil of approximately  $L = 76$  mH, which is close to the experimentally determined value of 77 mH.

### V. THE DRIVE OF THE HIGH FREQUENCY HELMHOLTZ COILS USING THE RESONANCE TECHNIQUE

The direct drive is used only for 50 Hz. In order to obtain the extension of the frequency range in which this large HC system is operating, the resonance method is used, which is advantageous at higher frequencies in order to obtain the lowest driving power [5].

Basically, series, parallel or series-parallel resonance can be used, with both series and parallel connection of HC coils. Fig. 16 describes all possible configurations that can be used to achieve resonance at higher frequencies. The choice of one or the other depends on the parameters of the HC system.

Next, some of these configurations are simulated in the LT Spice software to determine the resonance frequency and the current passing through the HC which corresponds to that frequency.

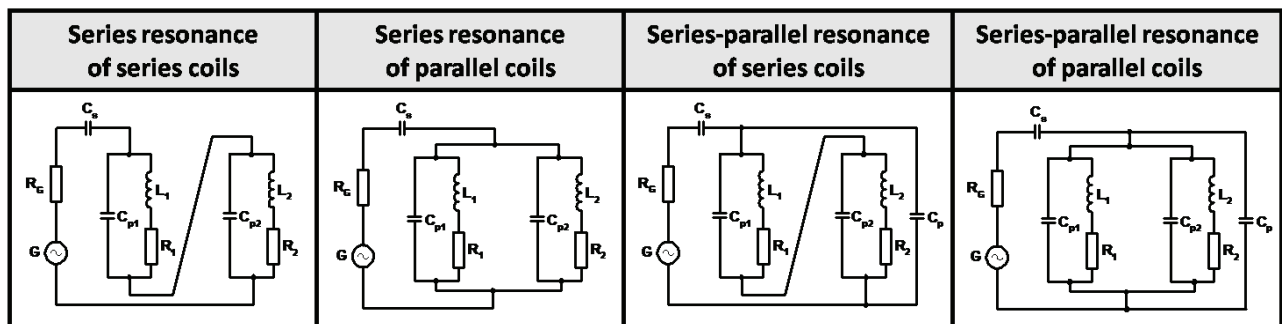
The electrical parameters of the HC electrical circuit are the ones determined experimentally, and the HC equivalent circuit at high frequency (Fig. 14) was used.

Figs. 17 and 18 represent two examples of the HC system modeling by the resonance technique. The electrical circuits are illustrated in the top left side, and the other sides illustrate the current passing through the source (and through the series connected capacitor)  $I_{C_s}$ , the current passing through the inductance  $I_{L_1}$ , and the one through the equivalent parasitic capacitance  $I_{C_p}$ , respectively. The maximum coil current at 500 Hz and 5 kHz, respectively is noted for both circuits.

The advantage of series connection for HC coils is that they are crossed by the same current.

A different  $C_s$  capacitor connected in series with the HC equivalent circuit was used in order to achieve the desired resonance frequency.

Another result of the simulations is the calculation of the rated power of the used amplifier at different resonant frequencies: e.g. 15 W at 500 Hz and only 5 W at 5 kHz (depending on the magnetic induction required in the calibration process). Thus a 25 W power amplifier fully covers the needs for the usual calibrations made with this HC system.



$$L_1 = L_2 ; R_1 = R_2 ; C_{p1} = C_{p2}$$

Fig. 16. Resonant configuration to supply HC Coils.

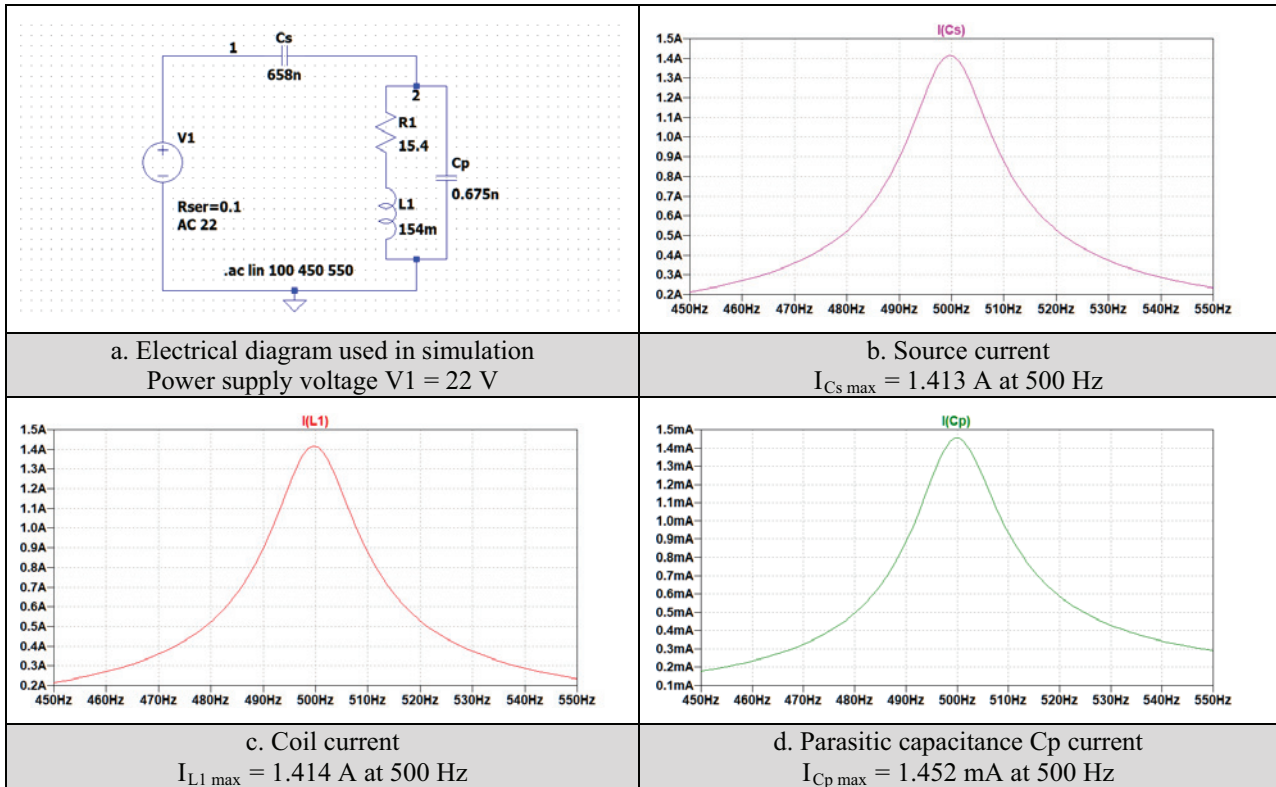


Fig. 17. Simulation of 500 Hz series resonance applied to the HC:  
a) electrical circuit; b) the source current; c) the coil current; d) the parasitic capacitance current.

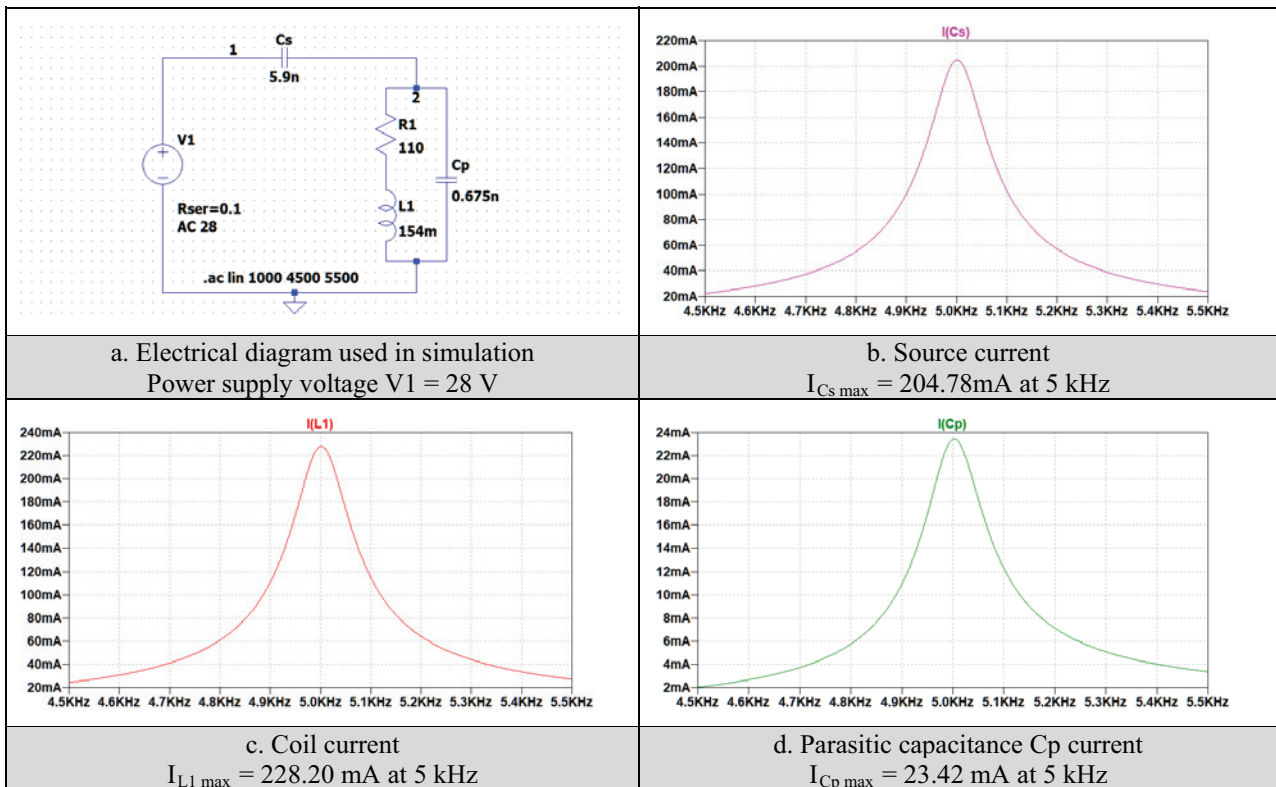


Fig. 18. Simulation of 5 kHz series resonance applied to the HC:  
a) electrical circuit; b) the source current; c) the coil current; d) the parasitic capacitance current.

## VI. EXPERIMENTS AND CALIBRATIONS

The measuring instrument used for calibration is the EFA-1 transfer standard [17] - a magnetic field analyser with internal three-axis B sensor that was previously calibrated at PTB Germany. This device performs measurements in the range from 5 Hz to 32 kHz (3 dB).

EFA-1 was arranged so that the field sensor was placed at the origin of the HC coordinate system. In order to determine the precise positioning of the field sensor, the anti-HC mounting is used. An anti-HC is the same HC, except the current in the two coils flows in opposite directions, similar to a gradiometer configuration (differential connection). At the centre point ( $x = 0, y = 0, z = 0$ ), the magnetic field must be equal to zero. In our experiment for  $I_L = 0.4$  A, the correction is  $5 \mu\text{T}$ .

Self-developed software [18] is used to check the uniformity of the magnetic field generated by the HC using the transfer standard. The magnetic induction is measured with the EFA-1 transfer standard and the electric current passing through the Helmholtz coils is determined by measuring the voltage drop across a shunt, with a Keythley 2000 multimeter. In order to increase the measurement accuracy, ten readings were performed on both devices, and the average value and the standard deviation are computed. The graphical interface of the employed software is illustrated in Fig. 19, while the result of the calibration of a magnetic field probe (EFA 300) is shown in Fig. 20.

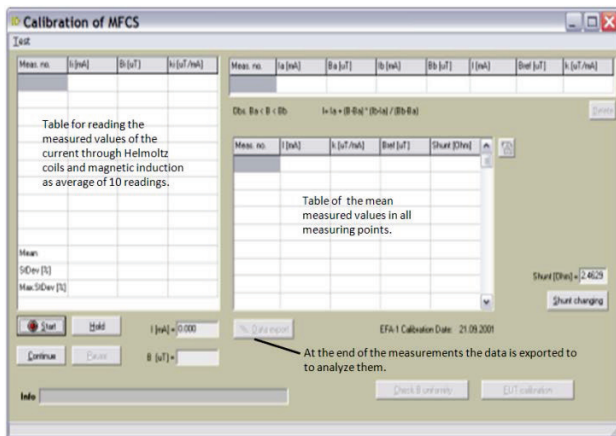


Fig. 19. Graphical user interface of the software for used checking the magnetic field uniformity.

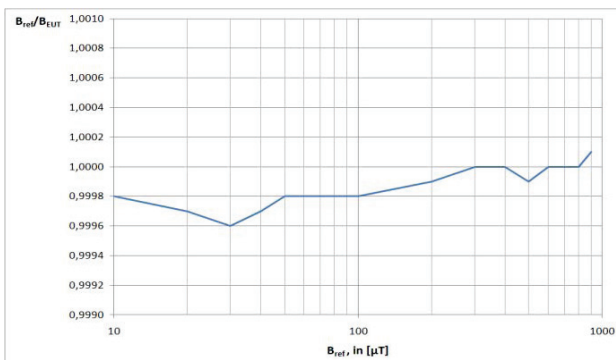


Fig. 20. Calibration result: ratio EFA-1/EFA-300.

The measurements included in Table 4, corresponding to the series resonant circuit were performed in order to verify the simulation results. As it can be noticed, the voltage drop across the coils  $U_L$ , at higher frequencies represent an important limiting factor (e.g. 4 V/turn at 5 kHz for a total applied voltage of 1100 V).

TABLE IV.  
THE MEASURED VALUES IN THE SERIES RESONANCE CIRCUIT.

$f$ [Hz]	50	673	1213	2460	5230
$I_L$ [A]	0.4	0.4	0.4	0.4	0.2
$B$ [ $\mu\text{T}$ ]	103	103	103	103	52
$U_L$ [V]	21	281	515	1004	1100

## VII. CONCLUSIONS

A request from industry customers to calibrate magnetic field sensors for operating frequencies up to 10 kHz led the authors to verify the extent to which the existing Helmholtz coil system at ICMET Institute could be used for this purpose. This system with  $1 \times 1\text{m}$  rectangular coils and multilayer solid copper wire winding was built and certified only for the working frequency of 50 Hz.

The paper demonstrates that the original HC system can operate without any modification at frequencies at least 100 times higher than the frequency for which it was built.

It determines the magnetic field generated by a HC system fulfilling the Helmholtz condition and its uniformity. The analytical calculation of the field uniformity results in a longitudinal zone of approximately 200 mm on the coils axis. By using numerical calculations based on FEM Maxwell software determines a field uniformity volume for a relative deviation of 1, 2 and 3 %. For a relative deviation of 2 % taken as a reference, the working volume is: 180 mm on the coils axis (longitudinal axis OY)  $\times$  300 mm on the transversal axis (OX),  $\times$  100 mm on the vertical axis (OZ), an acceptable volume for the calibration of many magnetic field sensors.

It can be noted that the vertical dimension of the field uniformity volume is smaller than the other dimensions – this is due the wires connecting the two HC coils, which were carrying currents of opposite directions.

By knowing the spatial distribution of the field deviation relative to the centre value, a field correction can be applied for sensors exceeding the uniformity volume. The experimenter can apply the correction by performing the field integration from the system centre to the longitudinal extremity.

The performed experiments aimed on the one hand to confirm the analytical and numerical results for the structure of the magnetic field and on the other hand to identify the parameters of the HC system in the extended frequency range initially proposed.

Some of the important results presented in the paper are:

- the comparison of the HC coils self inductance: FEM method vs measurement (76 vs 77 mH);
- the measurement in the frequency domain of all system parameters with an unique device of the Vector Network Analyzer type;

- the determination of the resonant frequency (15.6 kHz) of the HC system which makes possible measurements up to about 10 kHz;
- the application of the series resonance method that ensures equal currents through the two coils and reduces the necessary excitation power;
- the exact determination of the true magnetic midpoint of the HC system taking into account its inherent constructive imperfections.

**Source of research funding in this article:** Research program of the Military Technical Academy, George Cosbuc, Bucharest, Romania.

Contribution of authors:

First author – 50%

First co-author – 10%

Second co-author – 10%

The third co-author – 10%

The fourth co-author – 10%

The fifth co-author - 10%

Received on July 10, 2020

Editorial Approval on November 17, 2020

#### REFERENCES

- [1] DKD (Deutsche Kalibrierdienst) Calibration Certificate DKD-K-18701,1997, Renewed 2009.
- [2] W. M. Frix, G. G. Karady, and B. A. Venetz, "Comparison of calibration systems for magnetic field measurement equipment", *IEEE Trans. Power Del.*, vol. 9, pp. 100–108, Jan. 1994.
- [3] H. Zijlstra, *Experimental Methods in Magnetism*, vol 2. Measurement of magnetic quantities, North-Holland Publishing Company- Amsterdam, 1967.
- [4] G. Crotti, M. Chiampi, and D. Giordano, "Estimation of Stray Parameters of Coils for Reference Magnetic Field Generation", *IEEE Trans on Magnetics*, Vol. 42, No. 4, pp. 1439-1442, April 2006.
- [5] A. Marinescu, I. Dumbravă, I. Pătru, A. Scornea, "Resonant power supply for Helmholtz coil system for the calibration of magnetic field sensors to frequencies of up to 10 kHz", CEM Workshop, Craiova, 2016.
- [6] T. Tsz-Ka Li, Tri-axial Square Helmholtz Coil for Neutron EDM Experiment, The Chinese University of Hong Kong, Hong Kong, China, Aug. 2004.
- [7] O. Baltag, D. Costandache, and M. Rau, Bioelectromagnetism laboratory - case study, 4th Int. Symp. on Electrical and Electronics Engineering (ISEEE), Galati, Oct. 2013.
- [8] D. Costandache, A. Banarescu, O. Baltag, I. Rau, M. Rau, and S. Ojica, "Dynamic Shielding in Biomagnetism", International Conference on Advancements of Medicine and Health Care Through Technology - IFBME Proc., vol. 26, pp. 121-124, Cluj Napoca, Sept. 2009.
- [9] R. Bargallo, Finite Elements for Electrical Engineering. Barcelona, Spain: Universitat Politecnica de Catalunya, 2006.
- [10] S. Humphries, *Finite-element Methods for Electromagnetics*, Albuquerque, SUA, New Mexico, 2010.
- [11] C. Racasan, A. Racasan, V. Topa, and C. Munteanu, *Numerical Modeling of the Electromagnetic Field (in Romanian)*, Casa Cartii de Stiinta, Cluj-Napoca, 2007.
- [12] F. Enache, Gh. Gavrilă, and E. Cazacu, "Study of the uniform magnetic field domains (3D) in the case of the Helmholtz coils", *Rev. Roum. Sci. Techn. – Électrotechn. et Énerg.*, vol. 53, no. 2, pp. 189–197, 2008.
- [13] O. Baltag, G. Rosu, and M. Rau, "Magnetic field of parallel and twisted wire pairs," the 10th Int. Sympos. on Advanced Topics in Electrical Engineering, Bucharest, Romania, 2017, pp. 324-329. doi: 10.1109/ATEE.2017.7905020.
- [14] N. Nouri and B. Plaster, "Comparison of magnetic field uniformities for discretized and finite-sized standard, solenoidal, and spherical coils," Nuclear Instruments and Methods in Physics Research Section A: Accelerators, Spectrometers, Detectors and Associated Equipment, vol. 723, pp. 30–35, 2013.
- [15] P. Koss, C. Crawford, G. Bison, E. Wursten, M. Kasprzak, and N. Severijns, "PCB Coil Design Producing a Uniform Confined Magnetic Field", *IEEE Mag. Let.*, vol. 8, 2017. doi: 10.1109/LMAG.2017.2701771.
- [16] A. Marinescu, I. Dumbravă, „Using VNA for IPT Coupling Factor Measurement”, in *IEEE – PEMC, Varna*, 2016.
- [17] EFA1 User Manual [Online]. Available: <http://www.narda-sts.us>
- [18] I. Dumbravă, A. Marinescu, G. Mihai, A. Scornea, "Laboratory for Magnetic Field Probes Calibration", SICEM Symposium, Bucharest, 2002.

# Wireless Remote Control for the Anti-Hail Missiles Launch Ramp Positioning System

Sorin Stepan, Gheorghe Manolea\*

Conestoga College, Ontario, Canada, e-mail: sostepan@yahoo.com

\* University of Craiova / Department of Electromechanical, Environmental and Applied Informatics, Craiova, Romania  
e-mail: ghmanolea@gmail.com

**Abstract** – This paper describes a wireless remote control designed for the positioning system of the launching pad of anti-hail missiles used by the Romanian Anti-Hail System. The remote control operates in the ISM band of 2,4 GHz and was successfully tested on a simplified, small size, experimental model of the actual launch ramp. The remote control allows the operator to position the launch ramp on two axes, azimuth, and elevation, and fire the missiles, using momentary push buttons. A 16x2 characters LCD display indicates the current position of the ramp, and the presence and the type of the anti-hail missiles loaded on the ramp. The remote control was built using Arduino microcontrollers and radio frequency transceivers and uses two separate one-way transmitter-receiver radio channels. The simplified experimental model of the launch ramp features the main functional characteristics of the actual ramp and was designed and built for the purpose of testing the remote control, due to no access to the actual ramp, along with the intention of using it to train the Local Unit operating personnel during the off-season time. When designing and building the remote control and the experimental model of the ramp it was taken into consideration an easy implementation on the actual ramp, with minimal modifications.

**Cuvinte cheie:** *telecomandă, antigrindină, microcontroler, modul de emisie-recepție, lansator de rachete, sistem de poziționare*

**Keywords:** *remote control, anti-hail, microcontroller, transceiver, missiles launch ramp, positioning system.*

## I. INTRODUCTION

As a result of a research documentation and a visit to an anti-hail Zonal Command Center and an anti-hail Local Unit, it has been found that from an operational point of view, the anti-hail system in Romania uses launching ramps which can be positioned manually or by using temporary cables [1], [2], [3].

The wireless remote control described in this paper speeds up the process of ramp positioning, eliminates the inconvenience of placing and removing the temporary cables every season, and reduces the cost of the equipment by avoiding the cables.

## II. THE REAL MISSILES LAUNCH RAMP AND THE EXPERIMENTAL MODEL

### A. Description and parameters of the real ramp

The missiles launch ramps used by the Romanian Anti-Hail System are manufactured by SC

Electromecanica Ploiesti and are intended to ensure the launching of eight RAG-96 or RAG-96S type missiles (Fig. 1) [1]. Azimuth and elevation positioning with a precision of  $1.5^\circ$  is possible between  $0$  and  $360^\circ$  for the azimuth, and between  $20^\circ$  and  $85^\circ$  for the elevation respectively. The ramp uses synchronous motors with permanent magnets for azimuth and elevation positioning directions, driven by intelligent drives. The connection between the motors and the mechanical structure of the ramp is accomplished with worm gears and worm-wheel transmission which ensures one-way movement and mechanical locking [4].



Fig. 1. The missiles launch ramp used by the Romanian Anti-Hail System

### B. Description of the experimental model of the ramp

A simplified, small size, experimental model of the real ramp was built to test the remote control (Fig. 2) [5].

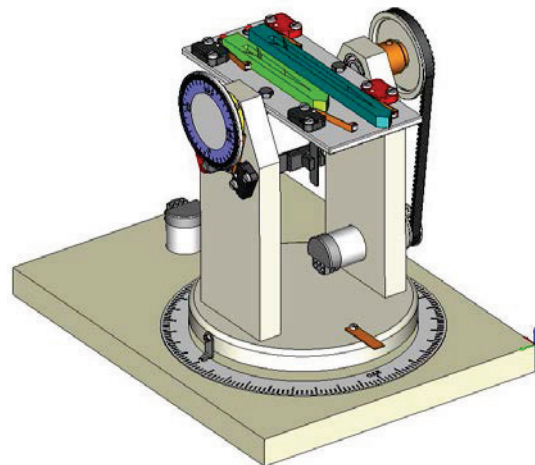


Fig. 2. The experimental model of the missiles launch ramp.

The experimental model features the two axes positioning of the actual ramp using two DC geared motors with encoders, controlled by a dual H-Bridge motor driver. The connection between the motors and the mechanical structure of the experimental model is achieved by gears and timing belts transmission. Feedback regarding azimuth and elevation coordinates is obtained from the pulses generated by the motor encoders. Optical sensors are used to set the home position on the two axes, and limit switches to indicate the presence and type of two missiles. A  $20^\circ$  to  $85^\circ$  interval for the elevation is set by two limit switches. The missiles firing is not possible outside this interval, and are simulated by two LEDs. The experimental model is electrically connected to the remote control receiver by six cables provided with DB9 connectors (Fig. 3).

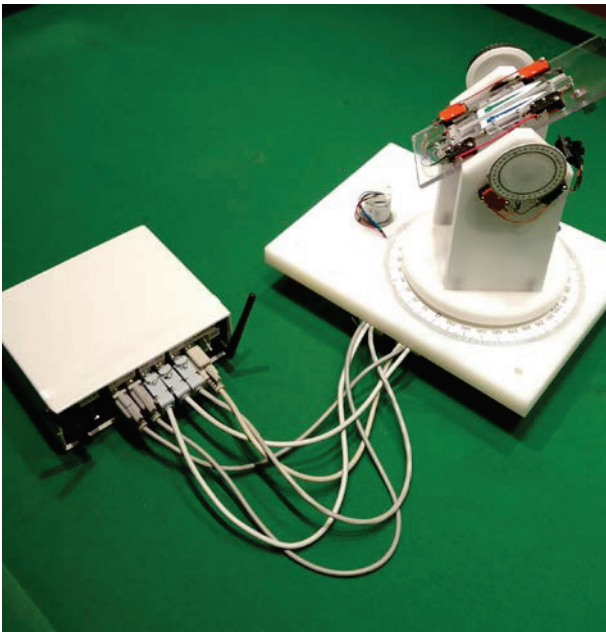


Fig. 3. The experimental model connected to the remote control receiver.

A 5V voltage from the remote control receiver box provides the power supply for the driver, motors, sensors, and LEDs on the experimental model.

When making the experimental model, it was taken into account that it retains the functional characteristics of the real ramp, so that after testing the remote control on the model, it can be implemented on the real ramp with minimal changes and the experimental model can be used for staff training in the active off-season.

The electrical schematic of the experimental model is shown in Fig. 4.

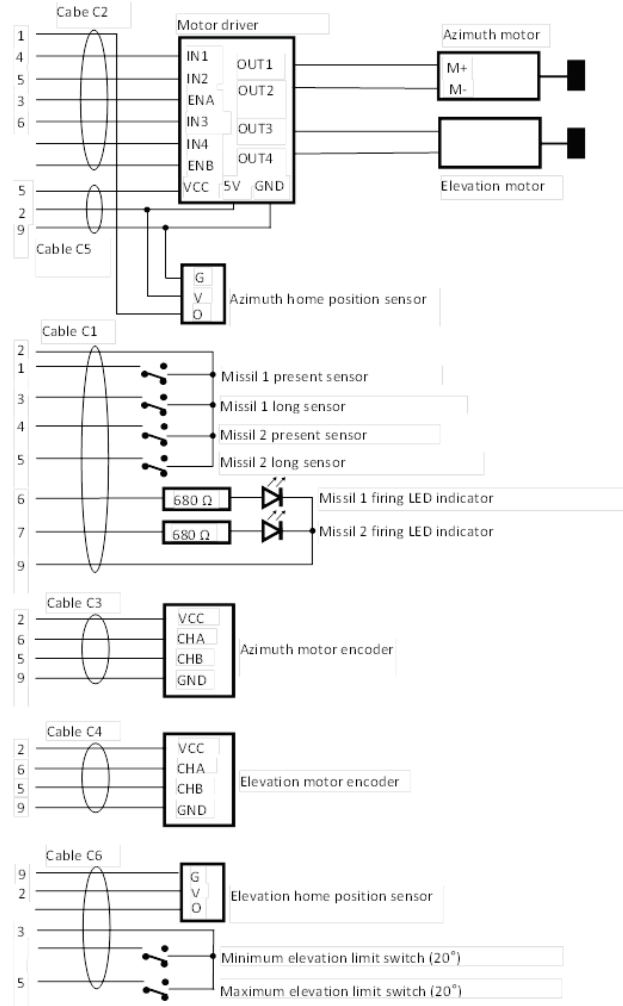


Fig. 4. Electrical schematic of the experimental model

### III. THE REMOTE CONTROL

#### A. Description and electrical diagram

The remote control uses two unilateral radio communication channels (transmitter-receiver) between Arduino type microcontrollers [6], [7], by using the NRF24L01 transmit-receive modules [8].

The first communication channel is sending commands from the operator to the ramp (move the ramp up, down, left or right, and fire the missiles), the second channel transmits data on the ramp to the operator (position, presence and type of missiles).

The block diagram of the first communication channel is that of Fig. 5.

This radio communication channel uses an Arduino Nano microcontroller at the transmitter and an Arduino Mega microcontroller at the receiver.